

Short communication

Battery impedance characterization through inspection of discharge curve and testing with short pulses

A. Tenno^{a,*}, R. Tenno^b, T. Suntio^c

^a Tallinn University of Technology, Department of Computer Control, Ehitajate tee 5, 19086 Tallinn, Estonia

^b Helsinki University of Technology, Control Engineering Laboratory, P.O. Box 5500, FI-02015 Espoo, Finland

^c Tampere University of Technology, Institute of Power Electronics, P.O. Box 692, FI-33101 Tampere, Finland

Available online 4 January 2006

Abstract

A simple method is proposed for battery impedance characterization at low frequencies (relevant to the electrochemical processes) and at higher frequencies (relevant to the double-layer process). The electrochemical impedance at very low frequencies is described using discharge curve information. This method makes it possible to distinguish between outwardly similar batteries that differ in backup times. The double-layer impedance at higher frequencies is characterized using short testing pulses. It is shown that the double-layer impedance of the negative electrode is observable in hertz range while the positive electrode is observable at the boundary to the millihertz range. The double-layer impedance of deeply discharged battery is observable at higher frequencies than the impedance of fully charged (or significantly discharged) battery because the electrodes are less overlapping in frequency and the spectrum shift to the higher frequencies is larger especially for the negative electrode.

© 2005 Elsevier B.V. All rights reserved.

Keywords: Battery; Lead-acid; Impedance; Estimation

1. Introduction

The purpose of the paper is to propose a simple method for battery impedance characterization at low frequencies (relevant to the electrochemical processes) and at higher frequencies (relevant to the double-layer process). The low frequency impedance will be characterized using discharge curves and the double-layer impedance using short-term current pulses injected similarly to the direct current method.

Battery impedance can be easily measured in hertz range [1,4]. This provides useful information on the double-impedance of the negative electrode. The positive electrode should be analysed at lower frequencies and the electrochemical processes at much lower frequencies. The electrochemical impedance spectroscopy [2,3] is designed to measure slow processes. These measurements are time-consuming and limited by several assumptions like the time-invariance of a battery during the measurements. This requirement is difficult to meet at low frequencies under discharge. For example, the measurement at 1 mHz requires 17 min of unchanged battery behaviour, which is problematic even under small test signal; it is unrealistic under

any discharge. For example, under relatively slow discharge of $C/I = 5$ h, the battery non-stationary behaviour is observable in the window of 10 s. Also, the test signal should be very small (to not corrupt the linear analysis), which increases the noise sensitivity of the measurements.

In this paper, the proposed method is not limited by the stationary or linearity requirements and is obviously not granted the benefits of linear analysis. The impedance spectrum depends on magnitude and form of the test signal applied, but allows for simple transformation of a discharge curve to an electrochemical impedance curve and in this way highlight differences of the outwardly similar batteries differing in available backup time.

The double-layer impedances of positive and negative electrodes are different; they can be calculated using another method of characterization based on short-term testing pulses. This method allows for simple transformation of the injected current and response voltage pulses in the double-layer impedance and in this way characterizes the positive and negative electrodes separately or together.

2. Electrochemical impedance

Battery electrochemical impedance can be calculated by the voltage and applied current using a Fourier transformation of

* Corresponding author.

E-mail address: ander.tenno@hut.fi (A. Tenno).

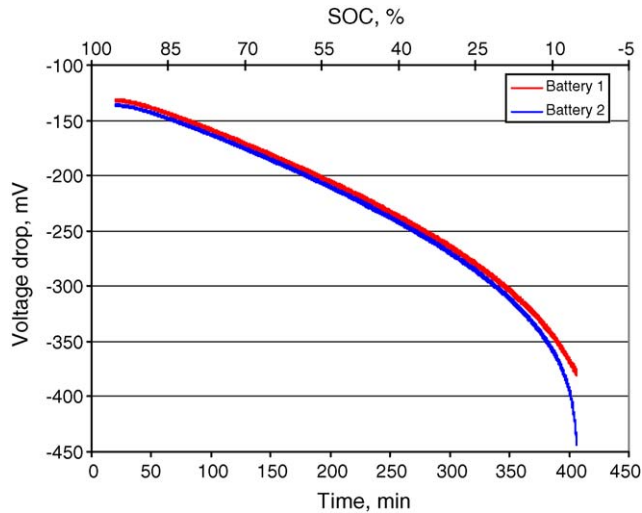


Fig. 1. Battery voltage drop during discharge.

these processes observed in certain period. This idea, justified in [5], is simplified in this paper to make the calculation procedure more practical.

2.1. Method

The discharge curves $v[0, t]$ of two batteries are shown in Fig. 1 as the voltage drop $v(t) = U(t)$ —OCV curves of float voltage $U(t)$ with respect to the open circuit voltage (OCV). They are relevant to $C/I_0 = 6$ h discharge with constant current $I_0 = -5$ A.

These curves' Fourier transformation is simpler if the voltage drop curve $v[0, t]$ is approximated with some simpler function, e.g. an exponential power series. It is simpler if the discharge curve is divided into several pieces and approximated piecewise as shown in Fig. 2.

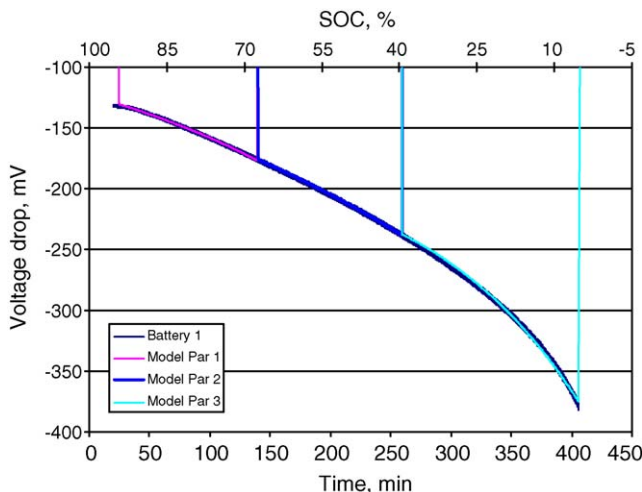


Fig. 2. Piecewise approximation of the voltage drop curve with model characterized with three sets of parameters.

In this case, the second-order exponential power series is a precise enough model

$$\Delta v(s) = V_0 \exp\{a_1 s + a_2 s^2\}, \quad (1)$$

where s is the time difference, $s = t - t_0$ with respect to the approximation point t_0 ; t the discharge time, $0 \leq t \leq T_0$; T_0 the discharge period between two of the approximation points (pulse width 2 h in Fig. 2); $\Delta v(s)$ the voltage drop, $\Delta v(s) = v(t) - V_0$ with respect to the initial voltage $V_0 = v(t_0)$; obviously, this difference for a voltage drop $v(t)$ and float voltage $U(t)$ is the same (V); a_1 and a_2 are the adapted coefficients to the discharge curve.

Theoretically, each piece of the discharge curve can be obtained as a response to the current pulse $I_0 = 5$ A inside the piece and 0 A outside. Thus, the voltage drop and current pulses are absolutely integrable functions, which is sufficient assumption for a Fourier analysis.

The Fourier transformations performed with respect to the voltage drop $v[t_0, t_0 + T_0]$ and current pulse $i[t_0, t_0 + T_0]$ curves and transformations divided with each other produce simple result [5]—the following spectral function for the electrochemical impedance:

$$Z_F = \left\{ \frac{\exp\{a_1 T_0 + a_2 T_0^2 - j\omega T_0\}}{a_1 + 2a_2 T_0 - j\omega} - \frac{1}{a_1 - j\omega} \right\} \times \frac{Rj\omega}{1 - \exp(-j\omega T_0)}, \quad (2)$$

where Z_F is the complex resistance (Ω); R the ohmic resistance at t_0 , $R = V_0/I_0$; I_0 the applied current: pulse amplitude (A); T_0 the forecast period: pulse width 2 h; j the imaginary unit, $j = \sqrt{-1}$; ω the angular frequency (rad s^{-1}), $\omega = 2\pi f$; f is the frequency (Hz).

The impedance can be calculated at any frequency from analytical formula (2). The impedance curve is close to the real axis at high frequencies in millihertz range because there are no changes in the electrochemical reaction relevant to this range (battery changes slowly during discharge). At low frequencies in millihertz range, the impedance curve is similar to the coth-based Warburg impedance (CPE-curve or almost vertical line) for positive electrode (or battery), and to the tanh-based Warburg impedance (semi-cycle) for negative electrode. In general, the impedance curve is a complex exponential function or logarithmic spiral, spinning in opposite directions for the positive and negative electrodes [5]. The positive electrode is affected more severely by the change of the acid concentration, inducing a counter-clockwise spin, while the spin of negative electrode is clockwise oriented. The impedance of the positive electrode is larger than the impedance of the negative electrode. Hence, it dominates in total for a battery. It is most logical to present the impedance curve in the microhertz range where most of the electrochemical reaction changes take place.

2.2. Results

The discharge curve in Fig. 2 can be represented as the electrochemical impedance shown in Fig. 3. It was calculated

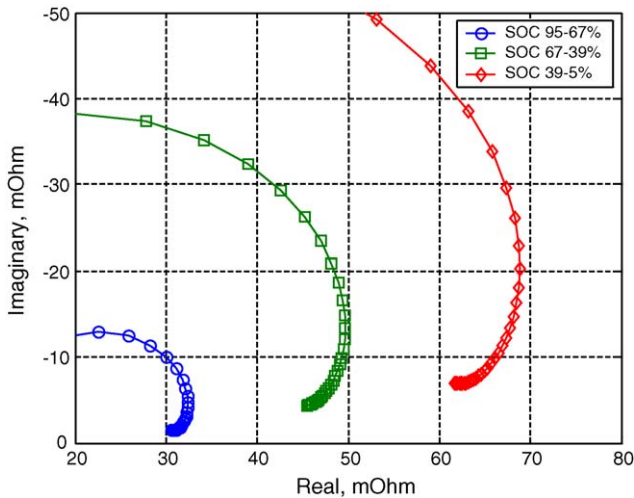


Fig. 3. Electrochemical impedance of Battery 1 calculated in the frequency range 1–70 μ Hz by the discharge curve in Fig. 2.

by (2) using adapted coefficients to the discharge curve of Battery 1.

The same calculation performed with respect to Battery 2 in Fig. 1 results in the electrochemical impedance shown in Fig. 4.

Battery 2 is weaker than Battery 1, which may also be concluded comparing the discharge curves in Fig. 1. The differences between the batteries are more visible by comparing the impedance curves in Figs. 3 and 4 than the discharge curves in Fig. 1. Therefore, the electrochemical impedance can possibly distinguish better between outwardly similar batteries differing in the available backup time, which is the main reason to use this method in practice.

3. Double-layer impedance

Battery double-layer impedance can be tested experimentally using short current pulses injected infrequently as in the direct current method.

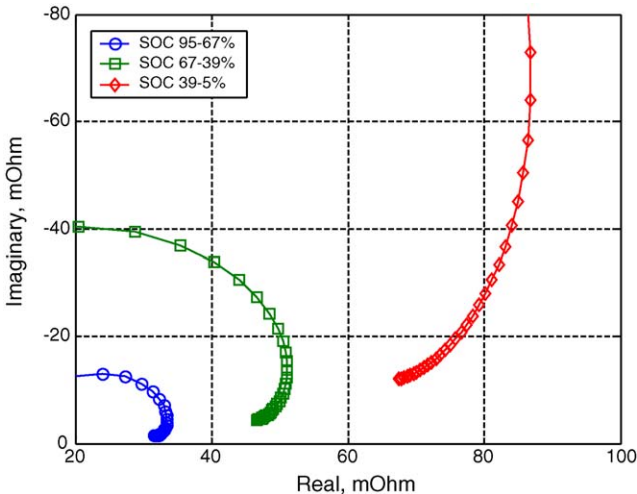


Fig. 4. Electrochemical impedance of a weaker Battery 2.

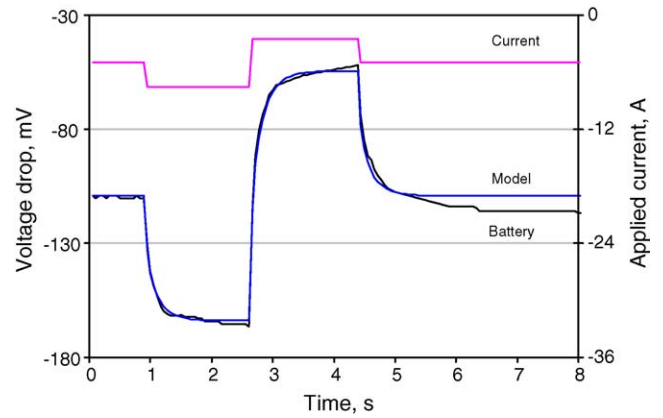


Fig. 5. Transient voltage drops of significantly discharged battery. Measured and model-predicted voltage.

3.1. Method

The transient voltage induced by the imposed square-wave current pulses can be represented with a two-rate differential model for the positive and negative electrodes [2]. This model solved analytically [2] can be represented as the sum of two exponential functions

$$\Delta u(s) = \Delta I_1 \left[R - R_1 \exp\left(\frac{-s}{R_1 C_1}\right) - R_2 \exp\left(\frac{-s}{R_2 C_2}\right) \right], \quad (3)$$

where s is the time difference, $s = t - t_0$ with respect to the approximation point t_0 ; t the testing time, $0 \leq t \leq T_1$; T_1 the testing period: pulse width 2 s in Figs. 5 and 6; $\Delta u(s)$ the voltage drop, $\Delta u(s) = u(t) - v(t_0)$ with respect to the initial drop $v(t_0) = I_0 R$ (approximation point) (V), the voltage drop $u(t)$ is defined as a response of voltage to the applied dc current I_0 and to the injected ac current pulse ΔI ; I the overall applied current, $I = I_0 + \Delta I$ (A); R the overall ohmic resistance, $R = R_0 + R_1 + R_2$, R_1 —charge-transfer resistance of positive or R_2 —negative electrodes, R_0 —total resistance of conducting elements, it includes resistance of electrodes and separator, grid resistance, intercell connector resistance and battery terminals resistance (Ω); C_1 is

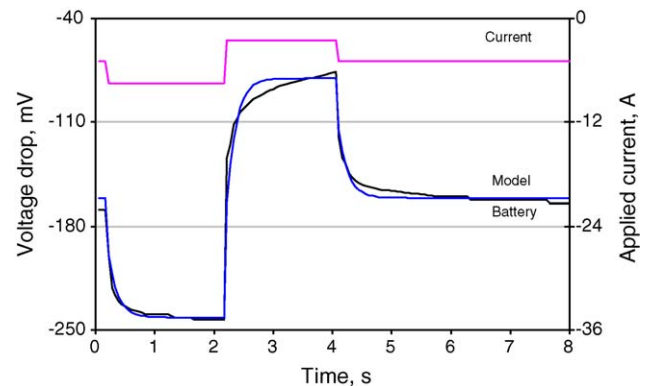


Fig. 6. Transient voltage drops of deeply discharged battery. Measured and model-predicted voltage.

Table 1
Model parameters: estimated by measurements

SOC (%)	R_0 (mΩ)	Positive electrode		Negative electrode	
		R_1 (mΩ)	C_1 (F)	R_2 (mΩ)	C_2 (F)
9	2	19	8	11	0.2
27	2	13	16	7	8

the double-layer capacitance of positive or C_2 —negative electrodes (F).

These parameters can be calculated as mean squares estimates, fitting the model (3) with a measured voltage drop curve. They depend on the state of charge (SOC) and are different for significantly discharged (SOC = 27%) and deeply discharged (SOC = 9%) battery (Table 1).

Their model fit is shown in Figs. 5 and 6, correspondingly.

The double-layer impedance can be calculated as a Fourier transformation $Z_{DL} = \mathbf{F}\{\Delta u(s) \times \Delta I^{-1}(s)\}$ of the voltage drop curve and current pulse curve. The resulting impedance can be represented as the following spectral function:

$$Z_{DL} = R + \frac{R_1}{1 + j\omega R_1 C_1} + \frac{R_2}{1 + j\omega R_2 C_2}. \quad (4)$$

The inductive components were not included in model (3) and not represented in spectrum (4). For this reason, the method is not applicable at higher frequency than 1 kHz. There may be also some inaccuracy in impedance spectrum at frequencies close to this limit.

3.2. Results

The double-layer impedance of the significantly discharged (SOC = 27%) battery is shown in Fig. 7; it was calculated by (4) for the positive and negative electrodes and in total for the battery. Impact of the positive electrode on the total battery impedance is larger than the impact of the negative electrode.

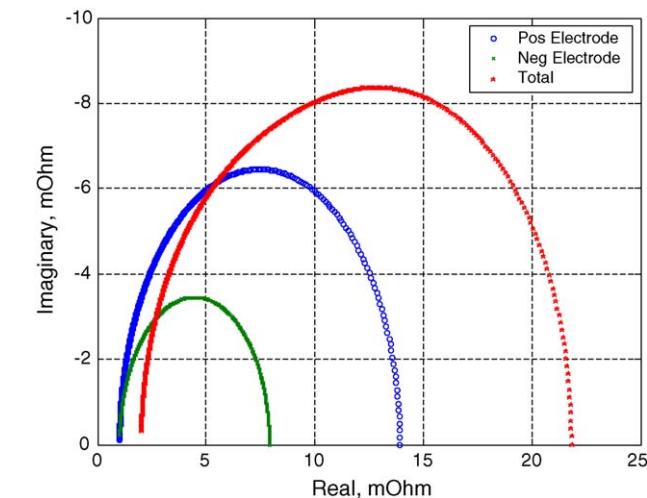


Fig. 7. Double-layer impedance of significantly discharged battery, shown for the positive and negative electrodes and in total for the battery.

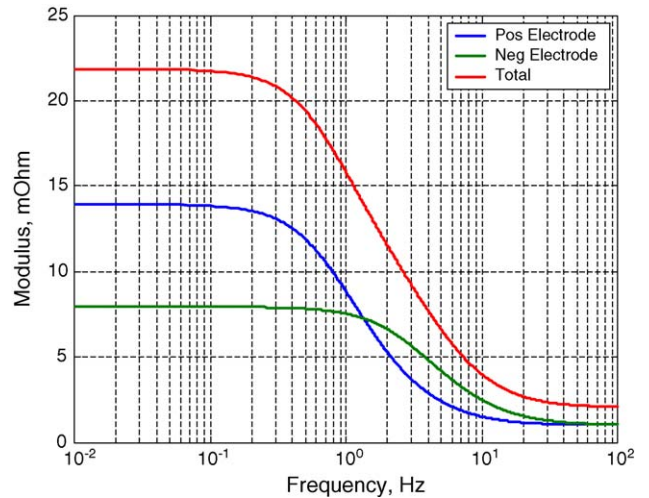


Fig. 8. Modulus of significantly discharged battery, shown for the positive and negative electrodes and in total.

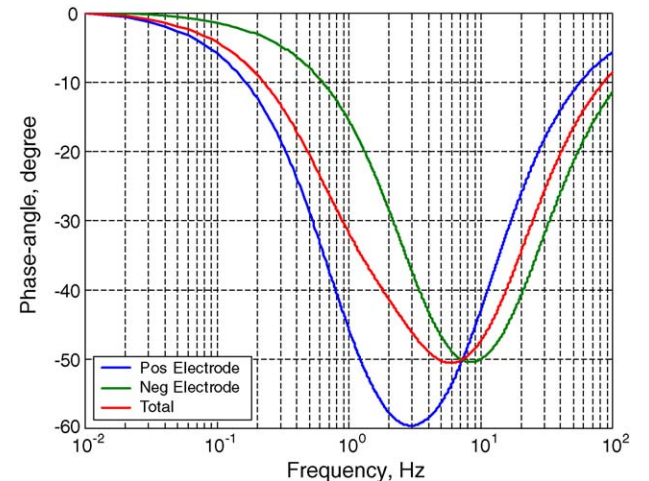


Fig. 9. Phase angle of significantly discharged battery, shown for the positive and negative electrodes and in total.

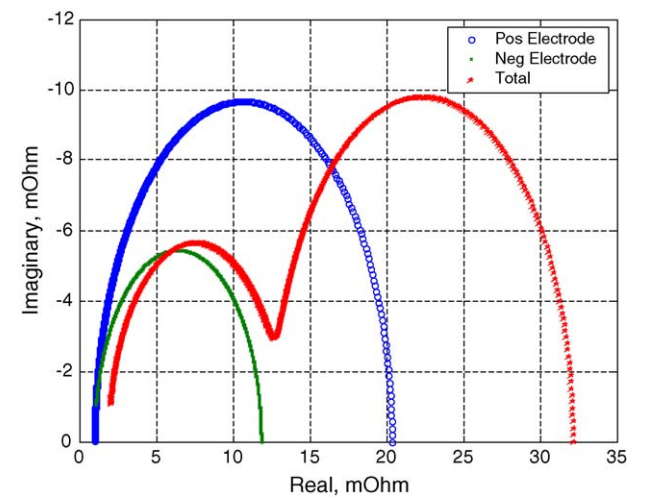


Fig. 10. Double-layer impedance of deeply discharged battery shown for the positive and negative electrodes and in total.

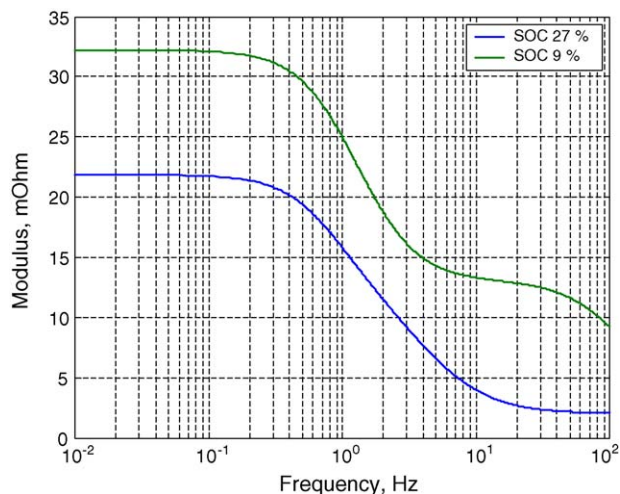


Fig. 11. Modulus of significantly discharged and deeply discharged batteries.

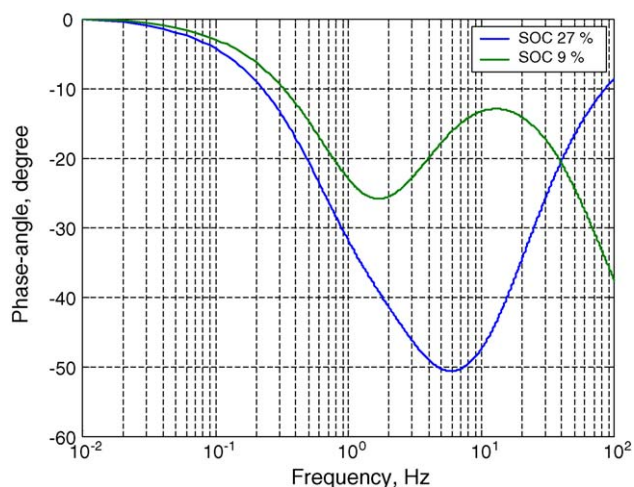


Fig. 12. Phase angles of significantly discharged and deeply discharged batteries.

This double-layer impedance is also represented as a spectrum of modulus and phase angle in Figs. 8 and 9.

The double-layer impedance of the negative electrode is clearly observable in hertz range; for the positive electrode and total impedance, it is observable at lower frequencies as shown in Figs. 8 and 9; for fully charged battery, it is observable at the boundary to the millihertz range or lower.

The behaviour of the deeply discharged (SOC = 9%) battery is different from the significantly discharged and fully charged batteries. The double-layer impedance is larger and the positive

and negative electrodes are less overlapping in frequency, which produces the double arc in the overall battery curve in Fig. 10.

There is also a large shift of the modulus and phase angle to the higher frequencies for the deeply discharged battery because spectrum shift is larger for the negative electrode in Figs. 11 and 12.

4. Battery overall impedance

Battery overall impedance of the electrochemical and double-layer processes can be calculated approximately by the superposition of both impedances

$$Z = Z_F + Z_{DL}, \quad (5)$$

where Z is the overall impedance; Z_{DL} the double-layer impedance; Z_F is the electrochemical impedance.

This approximation is justified by the nature of slow and fast processes. They are not overlapping in frequency [5]: the double-layer capacitance is an effective shunt for the Faradic current at the higher frequencies than 0.1 Hz.

5. Conclusion

It was shown that a battery can be characterized at very low frequencies with the electrochemical impedance calculated from the discharge curve and at higher frequencies with the double-layer impedance calculated from the voltage response pulses to short current pulses. The impedance characterization may give better information on the battery's internal capability to perform than the discharge curve directly. It may also be possible to characterize the battery performance using shorter discharge period (SOC $\geq 70\%$) than the complete capacity test when model-based methods are utilized.

References

- [1] D.O. Feder, T.G. Croda, K.S. Champlin, S.J. McShane, M.J. Hlavac, Conductance testing compared to traditional methods of evaluating the capacity of valve-regulated lead/acid batteries and predicting state-of-health, *J. Power Sources* 40 (1992) 235–250.
- [2] E. Karden, S. Buller, R.W. De Doncker, A method for measurement and interpretation of impedance spectra for industrial batteries, *J. Power Sources* 85 (2000) 72–78.
- [3] E. Karden, R.W. De Doncker, The non-linear low-frequency impedance of lead/acid batteries during discharge, charge and float operation, in: *Proceedings of the INTELEC'01*, 2001, pp. 65–72.
- [4] R.S. Robinson, On-line battery testing: a reliable method for determining battery health, in: *Proceedings of the IEEE INTELEC'96*, No. 4, 1996, pp. 654–661.
- [5] A. Tenno, R. Tenno, T. Suntio, Method for battery impedance analysis, *J. Electrochem. Soc.* 151 (6) (2004) A806–A824.